# Supporting Information for
# Optomechanical computing in liquid crystal elastomers

**Haley M. Tholen,*[a] Cedric P. Ambulo, [b,c] Kyung Min Lee,[b,c] Philip R. Buskohl,[b] and Ryan L. Harne*[a]**

[a]*Department of Mechanical Engineering, The Pennsylvania State University, University Park, PA, USA*

[b]*Materials and Manufacturing Directorate, Air Force Research Laboratory, Wright-Patterson Air Force Base, OH, USA*

[c]*Azimuth Corporation, Fairborn, OH, USA*

* *Corresponding authors: hmt5321@psu.edu, ryanharne@psu.edu*

## 1 Experimental characterization methods

### *1.1 Real-time infrared spectroscopy*

Real-time infrared (RTIR) spectra are obtained with a ThermoFisher Scientific Nicolet iS50 FTIR Spectrometer in the range of 600-4000 $cm^{-1}$ to provide insight into the efficiency of radical polymerization. Figure S1(a) displays incremental RTIR spectra over a period of 10 minutes that are recorded as the liquid crystal mixture is irradiated with 365 nm light at an intensity of 50 $mW/cm^2$. Series scans are taken at a rate of one scan per second. Two characteristic peaks are selected to represent acrylate functional groups from RM82, as shown in Figure S1(b) and Figure S1(c). The reduction in absorbance peak intensity indicates consumption of the corresponding functional groups as the reaction proceeds.

Acrylate conversion is determined using Equation S1 as a function of the decrease in the two peak areas, from 825 to 800 $cm^{-1}$ (Area 1) and from 1630 to 1644 $cm^{-1}$ (Area 2), where $A_{C=C(0)}$ is the absorption area of the peak at the start and $A_{C=C(t)}$ the absorption area of the peak by cure time.

$$\% DC = 100 - \left(1 - \frac{A_{C=C(t)}}{A_{C=C(0)}} * 100\right) \quad \text{(S1)}$$

Figure S2 shows the peak area curves and corresponding conversion curves for the two characteristic acrylate peaks. The change in area under the curve of each peak corresponds to the acrylic carbon−carbon double bond, which indicates the monomer conversion. The samples reach 80~90% conversion under the current polymerization conditions.

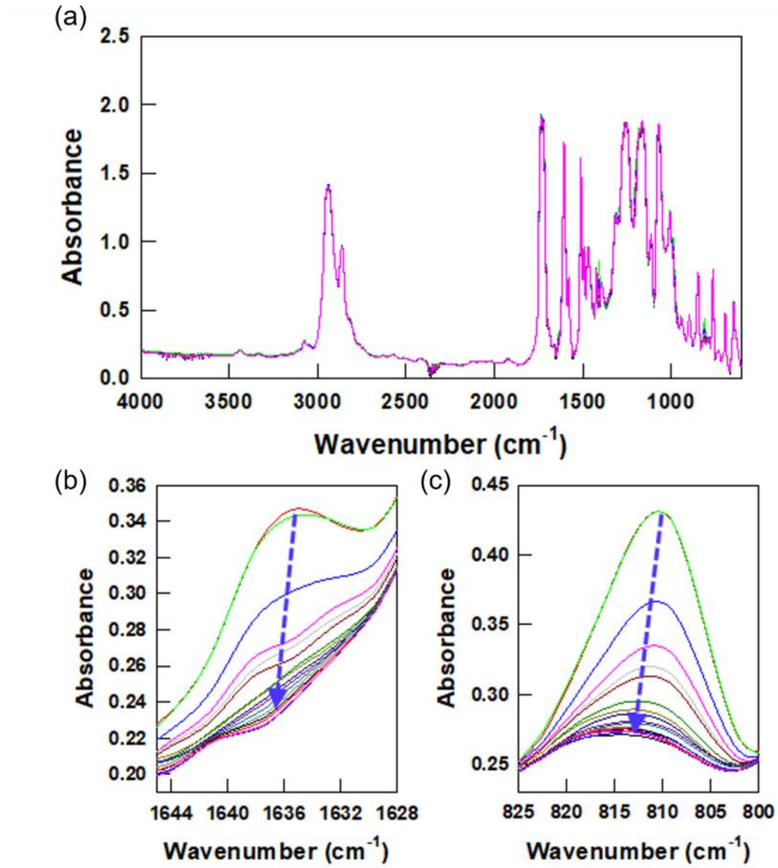


**Figure S1. (a) RTIR spectra of carbon black-embedded LCE during polymerization with selected characteristic peaks of (b, c) acrylate functional groups.**

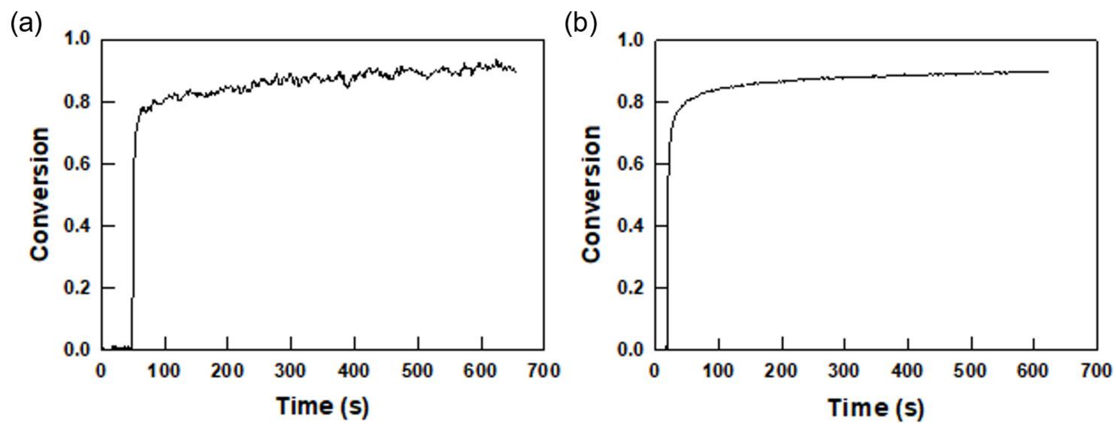


**Figure S2. Conversion plots for (a) Area 1 (1630-1644 $cm^{-1}$) and (b) Area 2 (800-825 $cm^{-1}$) RTIR spectra in Figure S1.**

### *1.2 Switching rate measurements*

The Micro-Epsilon optoNCDT ILDI 700-200 laser displacement sensor is used to measure vertical linear displacement, *d*, of NOT switches with various tip widths scaled with respect to the width of the conductive trace (600 µm). Figure S3 shows a schematic representation of the operation of laser displacement measurements used to characterize switching rate of each switch geometry. The NOT switch is chosen for measurements since each switch iteration begins in the same planar state and thus have nearly identical starting values. A Thorlabs M365L2-C1 collimated LED at 50 mW/cm$^2$ is toggled on and off for 10 cycles to expose the NOT switches. The exposure time is 5 seconds and the 10 second duration of the LED turned off is used to reset the switch. The time constant is derived from the displacement data in time is fitted with a first-order, exponential curve in the form $d = ae^{-\frac{t}{\tau}}$ during the actuation period of the NOT switch.

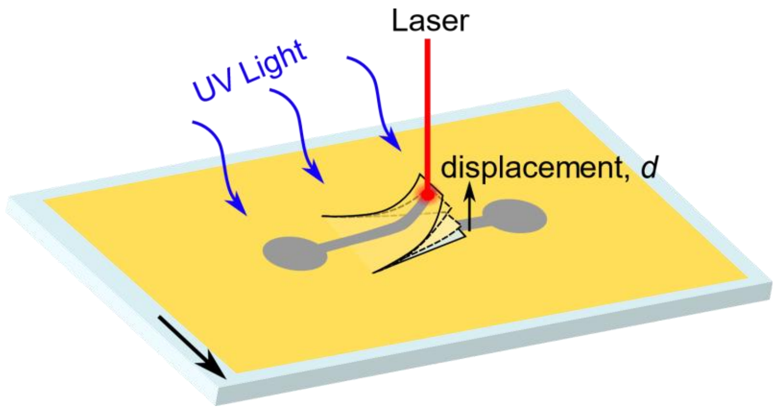


**Figure S3. Schematic of laser displacement measurements of a NOT switch. UV light irradiation actuates the switch to move upwards. When the UV light is switched off, the switch relaxes to its initial planar state.**

An empirical study is conducted to determine the optimal carbon black concentration with LCE samples with concentrations ranging from 0 wt% to 2 wt%. It was found that switching rate was not significantly affected by change in concentration in the chosen range. Perhaps an increased weight percentage would have a significant impact on switching rate, though too high of a carbon black concentration will drastically interfere with the mobility of the liquid crystals. Additionally, it was observed that samples with carbon black concentrations greater than 0.3 wt% resulted in visible striations and inhomogeneous spread of carbon black particles as the glass cell was filled.

### *1.3 Role of carbon black in computing LCEs*

An empirical study is conducted to determine the optimal concentration of carbon black in the polymer mixture comparing concentrations of 0.1 wt%, 0.3 wt%, 0.5 wt%, 1 wt%, and 2 wt%. It is observed that LCE films at the chosen thickness with carbon black content above 0.3 wt% showed obvious striations throughout the film, indicating an inhomogeneous spread of carbon black particles. Additionally, LCE films with 1 wt% and 2 wt% carbon black inhibited actuation, likely a result of carbon black particles becoming obstacles for effective mobility and shape change of individual liquid crystals. Thus, 0.3 wt% is chosen as the carbon black concentration for this study to ensure homogenous spread of carbon black particles, while also capitalizing on the photothermal effect as much as possible.

Since LCEs are innately temperature-responsive materials, it may be in question whether the computing LCE is actuated as a result of the photothermal effect or if heat emitted from the UV LEDs causes actuation. The AND and NAND logic gates are exposed to 200 mW/cm$^2$ of light and the maximum surface temperature is measured to be 24 ºC, increasing by only 2 ºC from room temperature. The 2-bit adder LCE is exposed to 330 mW/cm$^2$ of light and reaches a maximum surface temperature of 35 ºC. While it is expected that all samples will increase in surface temperature slightly as a result of the photothermal effect and exposure to high intensity light, the maximum temperatures reached remain well below the $T_{NI}$ of 105 ºC. This confirms that actuation occurs with irradiance and localized heat production of the carbon black particles and not due to an elevated thermal environment created by the UV light source.

## 2 2-bit adder states

The 2-bit adder combinational logic adds two 2-bit numbers, *A* and *B*, totaling a 3-bit sum, *Q*. The Boolean function, comprised of minterms containing the product (&) and sum (|) of all the input Boolean terms, is extracted from the truth table in Figure S4. The Quine-McCluskey algorithm (1) (2) is then applied to minimize this function, resulting in Equations S2 to S4. Here, each Boolean term in the minimized function corresponds to an individual Buffer ( $X_n$ ) or NOT ( $\overline{X}_n$ ) switch in the computing LCE. $Q_{Cout}$, $Q_{S2}$, and $Q_{S1}$ are realized as digital outputs in the experimental system, while inputs $A_1$, $A_2$, $B_1$, and $B_2$ correspond to optical information provided via a barcode pattern.

$$Q_{Cout} = \overline{A_1} \,\&\, B_1 \mid A_1 \,\&\, \overline{B_1} \tag{S2}$$

$$Q_{S2} = \overline{A_1} \,\&\, \overline{A_2} \,\&\, B_2 \mid \overline{A_1} \,\&\, A_2 \,\&\, \overline{B_2} \mid \overline{B_1} \,\&\, \overline{A_2} \,\&\, B_2 \mid \overline{B_1} \,\&\, A_2 \,\&\, \overline{B_2} \mid A_1 \,\&\, B_1 \,\&\, \overline{A_2} \,\&\, \overline{B_2} \mid A_1 \,\&\, B_1 \,\&\, A_2 \,\&\, B_2 \tag{S3}$$

$$Q_{S1} = A_2 \,\&\, B_2 \mid A_1 \,\&\, B_1 \,\&\, B_2 \mid A_1 \,\&\, B_1 \,\&\, A_2 \tag{S4}$$

Possible configurations for the 2-bit adder LCE are shown in Figure S4. Each computing LCE schematic provides information on the experimental realization of each configuration in the truth table. Purple bars represent strips of UV light using a barcode mask to selectively irradiate the LCE. UV light irradiation corresponds to a binary value of 1 for inputs $A_1$, $A_2$, $B_1$, and $B_2$, while a binary value of 0 indicates an absence of irradiation. After receiving the input signal, activated switches will connect and disconnect conductive traces throughout the network such that select conductive pathways are active, highlighted in cyan. To achieve a digital binary output value of 1, only one conductive pathway for each minterm, namely $Q_{Cout}$, $Q_{S2}$, or $Q_{S1}$, is required to be active. Each digital output signal corresponds to an LED light in the output display as seen in Video S1. A digital binary output of 1 results in the corresponding LED spot turning on, while the LED spot remains off when the digital binary output is 0. The $V_{CC}$ terminal is a low voltage signal that powers the LED lights for visualizing digital output signals.

| 2-bit Adder Truth Table | | | | | | |
|---|---|---|---|---|---|---|
| Inputs | | | | Outputs | | |
| $A_1$ | $B_1$ | $A_2$ | $B_2$ | $Q_{Cout}$ | $Q_{S2}$ | $Q_{S1}$ |
| 0 | 0 | 0 | 0 | 0 | 0 | 0 |
| 0 | 0 | 0 | 1 | 0 | 1 | 0 |
| 0 | 0 | 1 | 0 | 0 | 1 | 0 |
| 0 | 0 | 1 | 1 | 1 | 0 | 0 |
| 0 | 1 | 0 | 0 | 0 | 0 | 1 |
| 0 | 1 | 0 | 1 | 0 | 1 | 1 |
| 0 | 1 | 1 | 0 | 0 | 1 | 1 |
| 0 | 1 | 1 | 1 | 1 | 0 | 1 |
| 1 | 0 | 0 | 0 | 0 | 0 | 1 |
| 1 | 0 | 0 | 1 | 0 | 1 | 1 |
| 1 | 0 | 1 | 0 | 0 | 1 | 1 |
| 1 | 0 | 1 | 1 | 1 | 0 | 1 |
| 1 | 1 | 0 | 0 | 0 | 1 | 0 |
| 1 | 1 | 0 | 1 | 1 | 0 | 0 |
| 1 | 1 | 1 | 0 | 1 | 0 | 0 |
| 1 | 1 | 1 | 1 | 1 | 1 | 0 |

Purple bar denotes UV irradiation

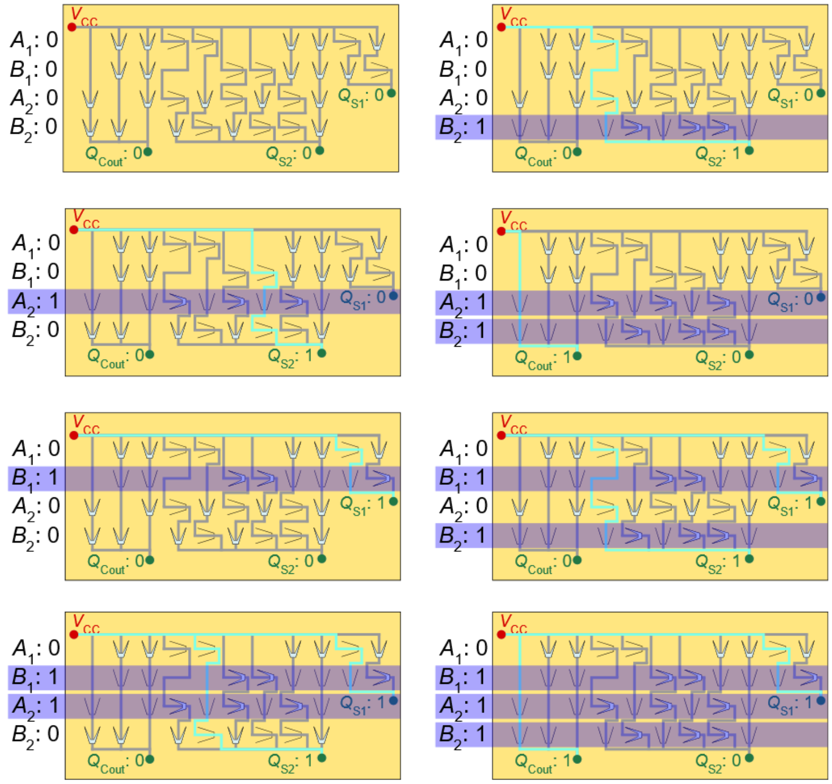


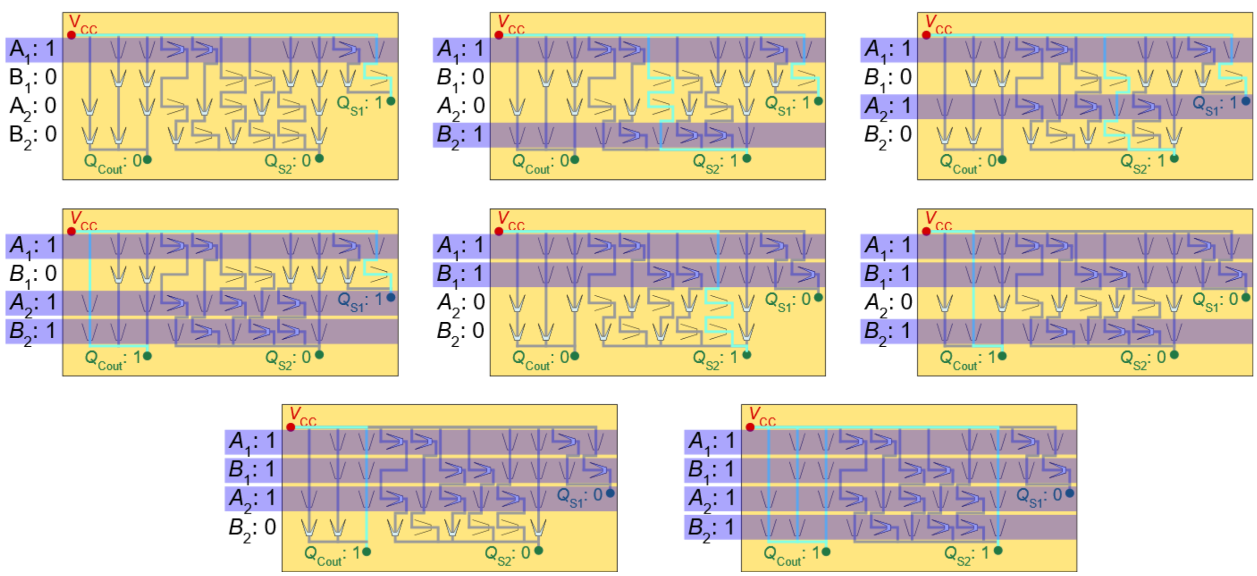


**Figure S4. 2-bit adder possible states with corresponding truth table. The purple bars on top of each sample indicate the irradiated bit(s) and the conductive trace(s) highlighted in cyan indicate the active pathway for each configuration.**

**References**


1. McCluskey EJ. Minimization of Boolean functions. The Bell System Technical Journal. 1956; 35: p. 1417-1444.

2. El Helou C, Grossmann B, Tabor CE, Buskohl PR, Harne RL. Mechanical integrated circuit materials. Nature. 2022; 608: p. 699-703.